



HAL
open science

Water/ice phase transition: The role of zirconium acetate, a compound with ice-shaping properties

Moreno Marcellini, Francisco M. Fernandes, Dmytro Dedovets, Sylvain Deville

► To cite this version:

Moreno Marcellini, Francisco M. Fernandes, Dmytro Dedovets, Sylvain Deville. Water/ice phase transition: The role of zirconium acetate, a compound with ice-shaping properties. *The Journal of Chemical Physics*, 2017, 146 (14), pp.144504. 10.1063/1.4979845 . hal-01520211

HAL Id: hal-01520211

<https://hal.sorbonne-universite.fr/hal-01520211v1>

Submitted on 10 May 2017

HAL is a multi-disciplinary open access archive for the deposit and dissemination of scientific research documents, whether they are published or not. The documents may come from teaching and research institutions in France or abroad, or from public or private research centers.

L'archive ouverte pluridisciplinaire **HAL**, est destinée au dépôt et à la diffusion de documents scientifiques de niveau recherche, publiés ou non, émanant des établissements d'enseignement et de recherche français ou étrangers, des laboratoires publics ou privés.

Water/ice phase transition: The role of zirconium acetate, a compound with ice-shaping properties

Moreno Marcellini, Francisco M. Fernandes, Dmytro Dedovets, and Sylvain Deville

Citation: *The Journal of Chemical Physics* **146**, 144504 (2017); doi: 10.1063/1.4979845

View online: <http://dx.doi.org/10.1063/1.4979845>

View Table of Contents: <http://aip.scitation.org/toc/jcp/146/14>

Published by the [American Institute of Physics](#)

Articles you may be interested in

[Perspective: Echoes in 2D-Raman-THz spectroscopy](#)

The Journal of Chemical Physics **146**, 130901130901 (2017); 10.1063/1.4979288

[Temperature of maximum density and excess properties of short-chain alcohol aqueous solutions: A simplified model simulation study](#)

The Journal of Chemical Physics **146**, 144503144503 (2017); 10.1063/1.4979806

[Perspective: Found in translation: Quantum chemical tools for grasping non-covalent interactions](#)

The Journal of Chemical Physics **146**, 120901120901 (2017); 10.1063/1.4978951

[Thermodynamic integration methods, infinite swapping, and the calculation of generalized averages](#)

The Journal of Chemical Physics **146**, 134111134111 (2017); 10.1063/1.4979493

[A Gaussian theory for fluctuations in simple liquids](#)

The Journal of Chemical Physics **146**, 134507134507 (2017); 10.1063/1.4979659

[Anomalous sound attenuation in Voronoi liquid](#)

The Journal of Chemical Physics **146**, 144502144502 (2017); 10.1063/1.4979720



**COMPLETELY
REDESIGNED!**

**PHYSICS
TODAY**

Physics Today Buyer's Guide
Search with a purpose.

Water/ice phase transition: The role of zirconium acetate, a compound with ice-shaping properties

Moreno Marcellini,¹ Francisco M. Fernandes,² Dmytro Dedovets,¹ and Sylvain Deville^{1,a)}

¹*Ceramic Synthesis and Functionalization Lab, UMR3080 CNRS/Saint-Gobain, 84306 Cavaillon, France*

²*Laboratoire de Chimie de la Matière Condensée de Paris, Université Pierre et Marie Curie, Sorbonne Universités, UMR7574, 4 Place Jussieu, 75005 Paris, France*

(Received 18 November 2016; accepted 15 March 2017; published online 13 April 2017)

Few compounds feature ice-shaping properties. Zirconium acetate is one of the very few inorganic compounds reported so far to have ice-shaping properties similar to that of ice-shaping proteins, encountered in many organisms living at low temperature. When a zirconium acetate solution is frozen, oriented and perfectly hexagonal ice crystals can be formed and their growth follows the temperature gradient. To shed light on the water/ice phase transition while freezing zirconium acetate solution, we carried out differential scanning calorimetry measurements. From our results, we estimate how many water molecules do not freeze because of their interaction with Zr cations. We estimate the colligative properties of the Zr acetate on the apparent critical temperature. We further show that the phase transition is unaffected by the nature of the base which is used to adjust the pH. Our results provide thus new hints on the ice-shaping mechanism of zirconium acetate. *Published by AIP Publishing.* [<http://dx.doi.org/10.1063/1.4979845>]

I. INTRODUCTION

Water molecules, albeit composed by 3 atoms only, show complex behaviors and anomalies. Several theoretical models were proposed to describe its physico-chemical properties:¹ each model can suitably describe only certain characteristics. For example, the nucleation of ice in water is difficult to predict. Indeed, the water/ice phase transition is a very common but still puzzling and challenging phenomenon.

The nucleation of ice crystals occurs both in vapor and in liquid phases. Although it is difficult to maintain large volumes of water below 0 °C without nucleation, a small volume can be held in supercooled conditions.² Pradzynski *et al.*³ found that at least 275 ± 25 water molecules are required to initiate the ice nucleation. The freezing of water in distinct physico-chemical conditions results in different ice patterns, such as those of snow crystals, or the dendritic and cellular structure grown in supercooled water.^{2,4}

The nucleation of water is hindered by solutes: NaCl in sea water, for instance, lowers the freezing point by ≈ -1.8 °C. Colloidal particles can also depress the freezing point of water.⁵ Ice is pure water. At the liquid-solid phase transition, water expels most of the ions and particles, which form brine channels between the ice crystals⁶ while releasing a latent heat $\Delta H_f = 333.6$ kJ/kg.² Nevertheless, some ions are easily incorporated in ice.

Zirconium acetate (ZrAc), a moderately water soluble crystalline Zr source, decomposes to zirconium oxide on calcination at high temperature.⁷ The physico-chemical processes leading to densification of liquid precursor solutions of ZrAc have been characterized by several methods.^{8–11} The behavior of ZrAc solutions at temperature below the water/ice

phase-transition was not investigated until ZrAc was used in ice-templating (also called freeze casting).¹² Ice templating is a material processing route based on the directional growth of ice crystals in colloidal suspensions and the successive removal of water by sublimation. The porosity is thus templated by the ice crystals. The templated microstructures, architectures, and properties are related to the morphology of ice crystals grown during freezing. In this process, ZrAc can be used either as an additive or as a ceramic precursor.

The use of ZrAc as an additive revealed its surprising ice-shaping properties.¹³ When a ZrAc solution is frozen in a narrow interval of pH (3.6–4.3) and concentration (≈ 9 to 22.6 g/l of Zr), faceted hexagonal ice crystals nucleate and grow along the direction of freezing (Fig. 1). Such faceting is similar to the effects of ice-shaping proteins (ISPs) that in fishes,¹⁴ insects,¹⁵ and plants¹⁶ hinder, for example, the growth of large ice crystals and stabilize ice crystals in specific shapes. ZrAc (and the less powerful Zr hydroacetate)^{13,17} is so far one of the very few inorganic compounds that functions like ISPs. However, ISPs work at concentration of μmol or lower (which corresponds, on average, to 0.1 to 1 g/L), whereas for ZrAc, the lowest reported concentration for effective ice shaping properties is ≈ 0.10 mol (9 g/l of Zr).¹³ The interactions of ISPs with ice are therefore probably much stronger than that of ZrAc.

To further understand the process that controls the growth of ice crystals in ZrAc solutions, we froze several ZrAc solutions, prepared in two different ways, and measured by Differential Scanning Calorimetry (DSC) the liquid/solid phase transition. From our results, we assessed the amount of ice in the sample and estimated the radius of interaction of Zr cations. We further show that the phase transition is a colligative effect of the Zr concentration, independently of the base used for pH correction.

a) sylvain.deville@saint-gobain.com

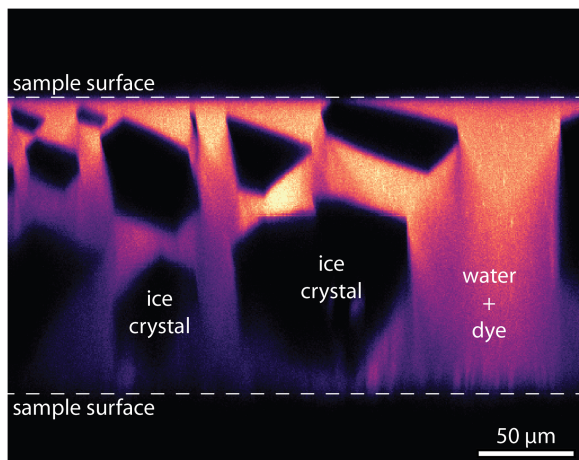


FIG. 1. Cryoconformal image of the cross section of ice crystals growing at $1 \mu\text{m/s}$ in the presence of zirconium acetate (Zr concentration: 18 g/l). The dye (sulforhodamine B) is expelled from the growing crystals, and the crystals appear thus as dark.¹⁸ The ice crystals are sharp and faceted. The cross section was obtained perpendicular to the direction of the temperature gradient along which the ice crystals grow.

II. SAMPLE PREPARATION

A solution of ZrAc (in-house preparation of Saint-Gobain¹⁹), with initial Zr concentration of 22.6 g/l (solution #1) and original pH = 2.6, was diluted in deionized water to obtain two other solutions with equivalent starting Zr concentrations of 13.3 g/l (pH = 3.2, solution #3) and 18 g/l (pH = 3.1, solution #2): each was prepared in two batches. The pH of one of the batches was then adjusted to pH = 4.0 ± 0.1 by adding NaOH powder and HCl solution at 37 wt. % (Sigma Aldrich): solutions #X(NaOH). This pH value is the optimal one to cause hexagonal ice-faceting while freezing the solution.^{13,17,20} The pH of the latter batch was carefully set, without overshooting, to pH ≈ 4 with TMAOH solution (tetramethylammonium hydroxide, Sigma Aldrich, concentration of 10 wt. % in water): solutions #X(TMAOH). TMAOH is a strong chaotrope molecule believed to weaken the hydrogen bonds network of water. It can entrap several molecules of water by hydrogen bonds^{21,22} producing clathrates.²³ Both Na^+ and Cl^- are in the middle of the Hofmeister series.^{24–26} The acetate group is more kosmotrope than Cl^- .²⁷ By probing two different sets of solutions, we can also assess whether the chaotrope/kosmotrope natures of the two bases affect the liquid/solid phase transition. The low initial concentration of the TMA-OH solution and its high $\text{pK}_b = 4.2$ caused large shifts in the final Zr concentration after the pH adjustment. The final concentration of the solutions adjusted with NaOH/HCl remained unchanged, see Table I. For each solution, we also prepared the corresponding reference solutions made up by a volume of water equivalent to the initial volume of the three solutions and the same amount of bases needed to adjust the pHs.

DSC measurements were carried out in N_2 atmosphere. The cooling/heating rate was set to $5 \text{ }^\circ\text{C/min}$ in the close cycle from $+40$ to $-80 \text{ }^\circ\text{C}$: for the #1(TMAOH) and #3(TMAOH) samples, we recorded additional thermograms at $1 \text{ }^\circ\text{C/min}$. We recorded two cycles per solution. The chosen freezing rate corresponds to ice shaping conditions used in freeze casting.

TABLE I. Samples and estimated Zr concentration.

Sample	NaOH/HCl (g/l)	TMA-OH (g/l)	Before pH adj.
#1	≈ 22.6	≈ 16.7	22.6
#2	≈ 17.7	≈ 14.5	18
#3	≈ 13.1	≈ 11.2	13.3

The data analysis was performed with the Universal Analysis 2000 (TA Instruments) software.

III. RESULTS AND DISCUSSION

The thermograms for the #X(NaOH) solutions are shown in Fig. 2. During the cooling semi-cycle, the freezing (critical) point is apparently depressed to temperatures $\leq -20 \text{ }^\circ\text{C}$ because the phase transition occurs in supercooled state, triggering an avalanche-like dendritic formation of ice crystals.⁴ The temperature increases during the phase transition for #3(NaOH). This artifact is due to the instrument not able to fully withdraw the latent heat. Likewise, the double peak for the #2(NaOH) is due to the spontaneous ice nucleation in supercooled conditions. Similar experiments on the #X(TMAOH) solutions give the results shown in Fig. 3. To understand whether the temperature scan rate causes a change in the melting temperature and the released heat, in Figure 4 we compared the thermogram of the #3(TMAOH) sample taken at the rates 5 and $1 \text{ }^\circ\text{C/min}$. We note that the temperature difference at the melting valley is significantly small despite the large difference in heat flow. Saeed *et al.*²⁸ have recently discussed how the difference in results can arise from using various temperature scan rates and amount of sample material. The thermal hysteresis observed can be related to different phenomena: the nucleation of ice is facilitated by nucleation points, such as, for example, dispersed particles, gas bubbles. If those lack, it is possible to bring water solutions in supercooled temperature. As soon as ice nucleates, it quickly releases the excess energy and ice crystals grow. If solutes are solved, then ice traps brines between the crystals.¹⁸ Melting, instead, looks alike a fully thermodynamic process. It is also possible that the small thermal hysteresis previously reported for ZrAc¹⁷

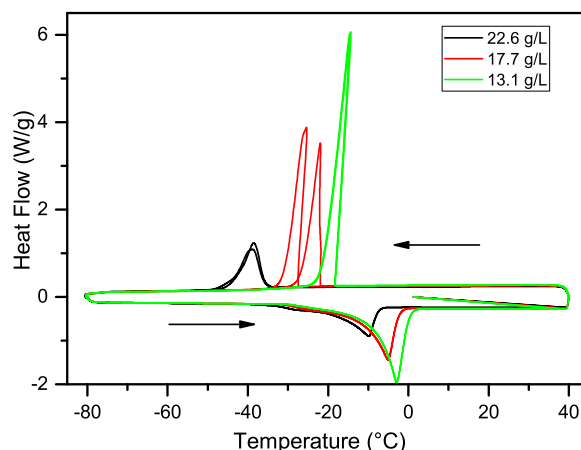


FIG. 2. Full thermograms of #X(NaOH) solutions. Arrows indicate the direction of the cycle.

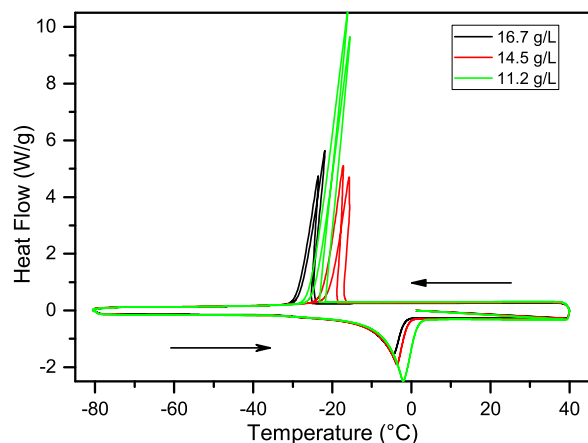


FIG. 3. Like in Fig. 2, thermograms for the #X(TMAOH) solutions. Similarly to the #X(NaOH) case, the apparent freezing temperatures correlate with the Zr concentration.

contributes in addition to the thermal hysteresis during freeze/thaw cycles reported here.

Hereby we define the apparent critical temperature T_c as the onset temperature of the solid/liquid phase transition. The onset temperatures are defined as the intersection, prior to the peak temperature, of the tangent of the peak with the extrapolated baseline and they should stay unchanged when the peak temperature shifts due to the change in heating rate or sample preparation. It usually is a more robust indicator of the thermal process by representing the starting point of the phase transition. Lower heating rate provides a more accurate measurement of the melting temperature, and larger heating rate allows us to measure the enthalpy of fusion with better accuracy. In our measurements, the larger is the heating rate the wider seems, in the temperature/heat-flow space, the phase transition. In Table II, we report the calculated results for T_c , T_{min} (T_{min} are the measured temperatures at the valley minima), and ΔH for two different temperature scan rates for #1(TMAOH) and #3(TMAOH) solutions. The temperature values of T_c for a consistent set of measurements and samples are reported in Table III and plotted in Fig. 5 with the corresponding results of reference solutions. These results tell us

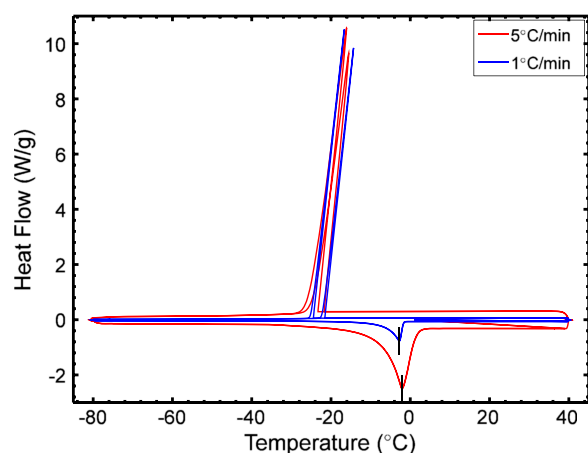


FIG. 4. Thermogram for the #3(TMAOH) solution at two temperature scan rates. Apparently, there is no significant difference between the two phase transitions. The vertical black bars are set at the valley minima.

TABLE II. Computed T_c , T_{min} , and ΔH for two solutions measured at two different temperature scan rates.

dT/dt (°C/min)	TMAOH sample	Cycle (g/l)	Zr (g/l)	T_c (°C)	T_{min} (°C)	ΔH (J/g)
1	#1	1	16.7	-9.79	-5.08	106.0
1		2	16.7	-9.84	-5.08	105.9
5		1	16.7	-10.24	-4.60	107.7
5		2	16.7	-10.25	-4.60	106.3
1	#3	1	11.2	-6.11	-2.76	171.5
1		2	11.2	-6.02	-2.74	169.7
5		1	11.2	-6.81	-2.06	168.7
5		2	11.2	-6.85	-2.10	168.4

that the apparent T_c is a colligative property of ZrAc concentration. For example, #2(NaOH) and #3(NaOH) share close concentrations with #1(TMAOH) and #2(TMAOH), respectively, and their T_c are quite similar. When the pHs of the original solutions are adjusted with NaOH/HCl, the large difference between the T_c of the samples and reference solutions hints to how strong the interaction between the solute (ZrAc) and the surrounding water shell is.

Various experimental results reported in past literature commonly agree that ZrAc and other Zr of monoprotic acid, in aqueous solution hydrolyze forming cyclic tetramers. The Zr ions are connected by hydroxo-bridges.²⁹⁻³¹ The stability of the cyclic tetramer has been also proven by computation.³² The polymerization reaction of tetramers into edge-sharing chains of tetramers³³ occurs depending on the concentration, the pH, and experimental conditions.

We thus hypothesize that the cyclic Zr tetramers organize, in water, as edge-sharing chains of tetramers, which were found both at room conditions³³ and at a pressure of 23 MPa.³⁴ The cyclic Zr tetramer is the universal structural motif: similar double chained Zr tetramer polymer has also been found at room temperature and pressure of 25 MPa in precursor for yttria-stabilized zirconia nanoparticles solved in methanol¹¹ and it also occurs in equilibrium with hexanuclear Zr acetate species.³¹ Dippel *et al.*¹¹ report a persistence order of the double chain of 10 Å, before a twist of the chain occurs, in pressure condition of 23 MPa.

Such chain structures decorated by acetate groups should resemble the one of ISPs from, for example, spruce budworm³⁵ or from winter flounder.³⁶ Similar idea has been recently proposed for a newly discovered organic compound that displays ice-shaping features.³⁷ These large structures (edge-sharing chains of tetramers) can interact with several water shells thanks to the ability of acetate groups to alter the hydrogen bonds network in the neighborhood. We hypothesize

TABLE III. Apparent T_c of ZrAc and reference solutions. (The latter in parentheses.)

Sample	Zr (g/l)	NaOH/HCl (°C)	Zr (g/l)	TMAOH (°C)
#1	22.6	-18.61 (-3.37)	16.7	-10.50 (-9.34)
#2	17.7	-11.45 (-3.58)	14.5	-8.91 (-5.62)
#3	13.1	-8.15 (-2.86)	11.2	-6.97 (-4.80)

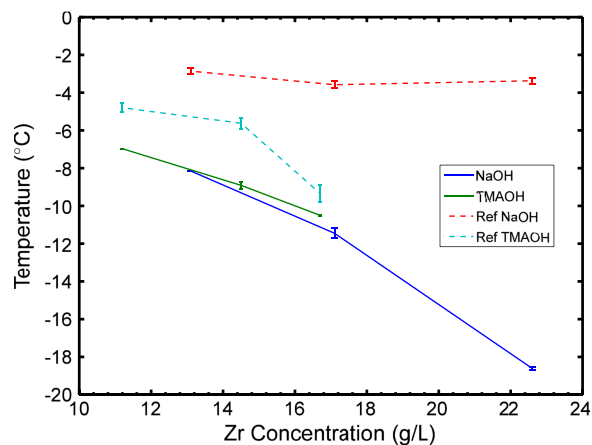


FIG. 5. T_c of the solutions. T_c is a colligative property of Zr concentration. (The lines are guide for the eyes.)

that likewise ISPs, these structures should adsorb onto the blooming ice crystals and cause their directional and faceted growth. Further microscopic measurements are needed to solve the topology of the organization of Zr ions under the conditions investigated here.

The latent heat L released at the phase transition depends only on the amount of water that participates in the phase transition. The ratio between the experimental and the tabulated ΔH_f value represents the amount of water that has taken part to the phase transition. Even though the enthalpy of fusion of water ΔH_f depends on the temperature³⁸ and within our temperature range, the change on ΔH_f is below 1%; ΔH_f decreases while increasing the pressure: from tabulated data,³⁹ we can estimate that the decrement is about 0.1% per 0.1 MPa; for a correct measurement of ΔH_f of the various solutions, we should properly proceed:⁴⁰ this is well beyond the scope of this work. In this way, we estimate that the systematic errors in our calculation of frozen water should not exceed 3%. These results, computed on the heating semi-cycle, are in Table IV and plotted in Fig. 6. Clearly the physico-chemical properties of the bases do not interfere with the phase transition. For example, the samples #2(NaOH) and #1(TMAOH) contain similar amount of ZrAc (17.7 g/l versus 16.7 g/l) and the ice content is similar. Thus, we may conclude that the thermodynamics of the process is due exclusively to ZrAc, strengthening the hypothesis that the ice-shaping properties of ZrAc are colligative. If we approximate the solutions as composed of water and ZrAc, we can estimate, from the amount of ice, how many molecules of water do not participate in the phase transition due to their interaction with the Zr cations. This approach is eased in the case of #X(NaOH) solutions, where the NaOH/HCl content is minimal. Thus, for the solution #1(NaOH), we estimate that 180 water molecules per

TABLE IV. Amount (percent) of frozen water in each sample. In parentheses the values for the reference solutions.

Sample	Zr (g/l)	NaOH/HCl (%)	Zr (g/l)	TMA-OH (%)
#1	22.6	19 (71)	16.7	35 (53)
#2	17.7	31 (74)	14.5	39 (62)
#3	13.1	40 (77)	11.2	51 (66)

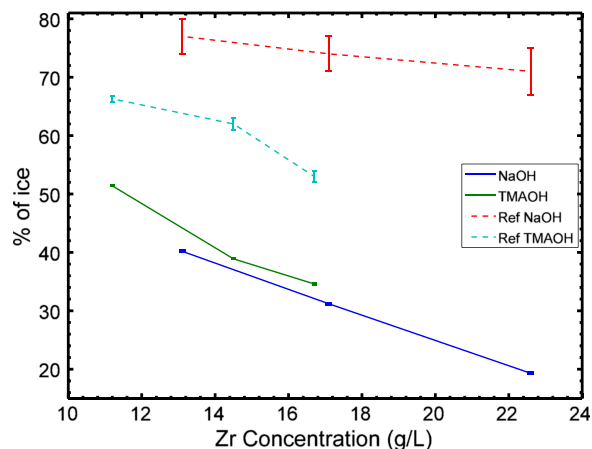


FIG. 6. Ice contents in the solutions. (The lines are guides for the eyes.)

TABLE V. Water molecules per Zr cation; radii of interaction per Zr cation; Zr concentration after phase transition in water. As Zr is expelled from the growing ice, its concentration in the liquid is higher after the phase transition.

Sample	H ₂ O molecules	Radius (nm)	Zr (g/l)
#1(NaOH)	180	1.74	27.9
#2(NaOH)	198	1.80	25.7
#3(NaOH)	232	1.89	21.8

Zr cation do not contribute to the phase transition. We can represent it as a sphere of radius $r \approx 1.74$ nm (see Table V). To give an idea of how large the sphere of interaction for Zr cations is, the Zr-Zr interdistance is ≈ 0.32 nm. For example, the TMAOH binds 25 water molecules by hydrogen bond.^{21,41} The percent of frozen water in Table IV represents, to a first approximation, the volume of ice. Since the ice turns into porosity in the final material, this volume is thus an indirect measurement of the overall porosity in ice-templated materials. While measuring the reference solutions, we noted a secondary peak at lower temperature occurring for the solution loaded exclusively with TMA-OH, Fig. 7. We believe that this extra phase transition could result from the formation of TMA-OH clathrates which have already been observed by Mootz and Seidel.²³

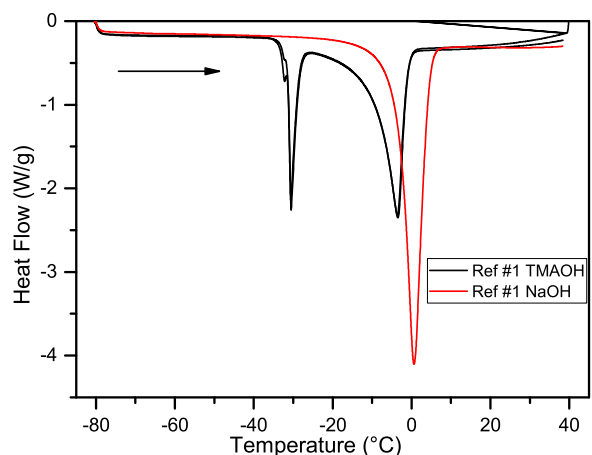


FIG. 7. DSC thermogram of the solid/liquid phase transitions for two reference solutions. Arrow indicates the direction of the cycle. Note the double melting peak for the solution loaded with TMA-OH.

IV. CONCLUSIONS

The freezing point T_c of the liquid/solid phase transition of water depends on the ionic content. We have shown that T_c is a colligative property of the ionic content of ZrAc, probably one of the very few inorganic compounds able to mimic the ice-shaping effects of ISPs. Further, the amount of ice depends on the concentration of Zr in solution, independently on how the pH of the solutions is stabilized. The chaotrope hydrophilic TMA-OH is very strongly influenced by the freezing process. The expected²³ clathrate organization of TMA-OH is destroyed by the presence of ZrAc. We have estimated the sphere of interaction of the Zr cations on water molecules. The Zr cations display a radius of interaction of few nm that comprises hundreds of water molecules. These results give a hint on the kosmotropic and hydrophilic strength of Zr or tetrameric chains, which should populate the solutions. The topology of Zr structures is really complex and it strongly depends on the chemical conditions. In the three cases investigated here, the number of water molecules that do not nucleate is different. This reinforces the hypothesis that the length of Zr supramolecular organization is inversely proportional to the concentration. The final concentration of Zr in the remnant liquid water should, thus, not be the same. Nevertheless, we can not exclude further effects due to the pH of the studied solutions. We think that terahertz spectroscopy⁴² experiments and *in situ* microscopic measurements could be used to better understand the ice-structuring mechanism of ZrAc.

ACKNOWLEDGMENTS

We acknowledge Dr. C. Noirjean for her comments on the manuscript. The research leading to these results has received funding from the European Research Council under the European Community's Seventh Framework Programme (No. FP7/2007-2013) Grant Agreement No. 278004, *FreeCo*.

¹ See http://www1.lsbu.ac.uk/water/water_models.html for information about the several parameterizations of water molecules generally used in Molecular Dynamic and Monte Carlo simulations.

² P. V. Hobbs, *Ice Physics*, Oxford Classic Texts in the Physical Sciences (Oxford University Press, 2010).

³ C. C. Pradzynski, R. M. Forck, T. Zeuch, P. Slavíček, and U. Buck, *Science* **337**, 1529 (2012).

⁴ A. Shibkov, Y. Golovin, M. Zheltov, A. Korolev, and A. Leonov, *Physica A* **319**, 65 (2003).

⁵ S. S. Peppin, J. A. W. Elliott, and M. Grae Worster, *J. Fluid Mech.* **554**, 147 (2006).

⁶ *The Geophysics of Sea Ice*, 1st ed., edited by N. Untersteiner (Springer, USA, 1986).

- ⁷ T. Tojo, T. Atake, T. Mori, and H. Yamamura, *J. Therm. Anal. Calorim.* **57**, 447 (1999).
- ⁸ J.-L. Tosan, B. Durand, M. Roubin, F. Chassagneux, and F. Bertin, *J. Non-Cryst. Solids* **168**, 23 (1994).
- ⁹ A. C. Geiculescu and H. G. Spencer, *J. Sol-Gel Sci. Technol.* **16**, 243 (1999).
- ¹⁰ A. George and P. T. Seena, *J. Therm. Anal. Calorim.* **110**, 1037 (2012).
- ¹¹ A.-C. Dippel, K. M. Ø. Jensen, C. Tyrsted, M. Bremholm, E. D. Bøjesen, D. Saha, S. Birgisson, M. Christensen, S. J. L. Billinge, and B. B. Iversen, *Acta Crystallogr., Sect. A: Found. Adv.* **72**, 645 (2016).
- ¹² S. Deville, *Adv. Eng. Mater.* **10**, 155 (2008).
- ¹³ S. Deville, C. Viazzi, J. Leloup, A. Lasalle, C. Guizard, E. Maire, J. Adrien, and L. Gremillard, *PLoS One* **6**, e26474 (2011).
- ¹⁴ J. G. Duman and A. L. DeVries, *Nature* **247**, 237 (1974).
- ¹⁵ C. A. Knight and J. G. Duman, *Cryobiology* **23**, 256 (1986).
- ¹⁶ M. Griffith, M. Antikainen, W.-C. Hon, K. Pihakaski-Maunsbach, X.-M. Yu, J. U. Chun, and D. S. C. Yang, *Physiol. Plant.* **100**, 327 (1997).
- ¹⁷ O. Mizrahy, M. Bar-Dolev, S. Guy, and I. Braslavsky, *PLoS One* **8**, e59540 (2013).
- ¹⁸ M. Marcellini, C. Noirjean, D. Dedovets, J. Maria, and S. Deville, *ACS Omega* **1**, 1019 (2016).
- ¹⁹ The ice-shaping properties of ZrAc are independent of the supplier.
- ²⁰ S. Deville, C. Viazzi, and C. Guizard, *Langmuir* **28**, 14892 (2012).
- ²¹ Y. Koga, P. Westh, K. Nishikawa, and S. Subramanian, *J. Phys. Chem. B* **115**, 2995 (2011).
- ²² E. J. Nilsson, V. Alfreðsson, D. T. Bowron, and K. J. Edler, *Phys. Chem. Chem. Phys.* **18**, 11193 (2016).
- ²³ D. Mootz and R. Seidel, *J. Inclusion Phenom. Mol. Recognit. Chem.* **8**, 139 (1990).
- ²⁴ Y. Zhang and P. S. Cremer, *Curr. Opin. Chem. Biol.* **10**, 658 (2006).
- ²⁵ K. D. Collins and M. W. Washabaugh, *Q. Rev. Biophys.* **18**, 323 (2009).
- ²⁶ A. A. Zavitsas, *Curr. Opin. Colloid Interface Sci.* **23**, 72 (2016).
- ²⁷ P. Lo Nostro and B. W. Ninham, *Chem. Rev.* **112**, 2286 (2012).
- ²⁸ R. M. Saeed, J. P. Schlegel, C. Castano, and R. Sawafta, *Int. J. Eng. Res. Technol.* **5**, 405 (2016); available at <http://www.ijert.org/view-pdf/14630/uncertainty-of-thermal-characterization-of-phase-change-material-by-differential-scanning-calorimetry-analysis>.
- ²⁹ A. Clearfield, *J. Mater. Res.* **5**, 161 (1990).
- ³⁰ C. Hagfeldt, V. Kessler, and I. Persson, *Dalton Trans.* **2004**, 2142–2151 (2004).
- ³¹ C. Hennig, S. Weiss, W. Kraus, J. Kretzschmar, and A. C. Scheinost, *Inorg. Chem.* **56**, 2473 (2017).
- ³² N. Rao, M. N. Holerca, M. L. Klein, and V. Pophristic, *J. Phys. Chem. A* **111**, 11395 (2007).
- ³³ M. Bremholm, H. Birkedal, B. B. Iversen, and J. S. Pedersen, *J. Phys. Chem. C* **119**, 12660 (2015).
- ³⁴ C. Tyrsted, N. Lock, K. M. Ø. Jensen, M. Christensen, E. D. Bøjesen, H. Emerich, G. Vaughan, S. J. L. Billinge, and B. B. Iversen, *IUCrJ* **1**, 165 (2014).
- ³⁵ E. K. Leinala, P. L. Davies, and Z. Jia, *Structure* **10**, 619 (2002).
- ³⁶ T. Sun, F.-H. Lin, R. L. Campbell, J. S. Allingham, and P. L. Davies, *Science* **343**, 795 (2014).
- ³⁷ R. Drori, C. Li, C. Hu, P. Raiteri, A. L. Rohl, M. D. Ward, and B. Kahr, *J. Am. Chem. Soc.* **138**, 13396 (2016).
- ³⁸ R. C. Dougherty and L. N. Howard, *J. Chem. Phys.* **109**, 7379 (1998).
- ³⁹ S. Denys, A. M. Van Loey, and M. E. Hendrickx, *Biotechnol. Prog.* **16**, 447 (2000).
- ⁴⁰ T. Asaoka, H. Kumano, M. Okada, and H. Kose, *Int. J. Refrig.* **33**, 1533 (2010).
- ⁴¹ Y. Koga, F. Sebe, and K. Nishikawa, *J. Phys. Chem. B* **117**, 877 (2013).
- ⁴² A. Shalit, S. Ahmed, J. Savolainen, and P. Hamm, *Nat. Chem.* **9**, 273 (2017).